Polymer bulk heterojunction solar cells: function and utility of inserting a hole transport and electron blocking layer into the device structure†‡

Yanming Sun,[a] Mingfeng Wang,[ab] Xiong Gong,[a] Jung Hwa Seo,[a] Ben B. Y. Hsu,[a] Fred Wudl[ab] and Alan J. Heeger[*a]

The function and utility of inserting an *in situ* polymerizable triphenylamine-containing polyperfluorocyclobutane (TPA–PFCB) as a hole transport and electron blocking layer into the structure of bulk heterojunction (BHJ) solar cells were demonstrated. The open-circuit voltage (V_{oc}) and short-circuit current (J_{sc}) increase, leading to BHJ solar cells with improved power conversion efficiency.

Solution-processed bulk heterojunction (BHJ) polymer solar cells (PSCs), comprising a phase separated mixture with interpenetrating networks of the conjugated polymers (electron donor) and fullerene derivatives (electron acceptor), are a focus of research directed toward low cost conversion of sunlight to electricity.[1–5] Several methods for improving the power conversion efficiency (PCE) of BHJ solar cells are known to be effective, including the design and synthesis of new low-band gap materials to harvest the solar spectrum more efficiently, thermal annealing and solvent annealing to improve the nanoscale morphology, and control of the morphology of polymer–fullerene blends by optimizing the processing conditions through the use of additives.[6–16]

Interface engineering is an alternative approach to improved performance. Following charge transfer and charge separation at the donor–acceptor interface, the holes and electrons are free to drift and diffuse along the conjugated polymer–fullerene interpenetrating networks to the appropriate electrodes where they are collected. The use of charge selective transport layers enables all the nanoscale solar cells within the BHJ material to be connected in parallel. Moreover, the use of charge selective transport layers breaks the symmetry and forces the photogenerated carriers to flow toward and be collected at the desired electrode (anode for holes and cathode for electrons). The use of charge selective layers can also improve the diode characteristics and thereby reduce the dark current. The latter is especially important for photo-detector applications,[17] where low dark currents are required for high detectivity.

The use of charge selective transport layers has proven to be a useful approach. Previous studies demonstrated that a thin titanium oxide (TiO_x) layer inserted between Al cathode and BHJ layer serves as a hole blocking layer and also acts as an "optical spacer," resulting in significant improvement in the efficiency and lifetime of the BHJ solar cells.[18–22] For indium tin oxide (ITO) as the anode, poly(3,4-ethylenedioxylenethiophene):polystyrene sulfonic acid (PEDOT:PSS) is commonly used as a passivationlayer to control the work function and improve the hole collection efficiency.[23–25] As a doped polymer, however, PEDOT:PSS does not function as a charge selective transport layer.[26] Here, we demonstrate triphenylamine-containing polyperfluorocyclobutane (TPA–PFCB) as a hole-transport and electron-blocking layer for polymer BHJ solar cells. TPA–PFCB was first used as a hole-transport layer in polymer light-emitting diodes (PLEDs).[27] Thus, we expect that a thin TPA–PFCB layer inserted between ITO and the BHJ layer can function as a charge selective hole transport and electron blocking layer. We find that compared with control solar cells, insertion of the TPA–PFCB layer causes both the open-circuit voltage (V_{oc}) and short-circuit current (J_{sc}) to increase, leading to enhanced efficiency.

The molecular structure of TPA–PFCB is shown in Scheme 1. TPA–PFCB can be polymerized *in situ* through thermal cyclo-dimerization at 225 °C for 45 min (under N_2). After polymerization, TPA–PFCB film is resistant to common organic solvents, such as toluene, chlorobenzene (CB) and dichlorobenzene (DCB). It is transparent over the entire visible region (see ESI‡, Fig. S1). The surface morphology of TPA–PFCB films after polymerization was investigated by atomic force microscopy (AFM). The surface roughness of TPA–PFCB/ITO was significantly less than that of ITO; the root mean square (RMS) roughness of TPA–PFCB film was 0.35 nm, while the RMS value of bare ITO was 0.60 nm (Fig. 1).
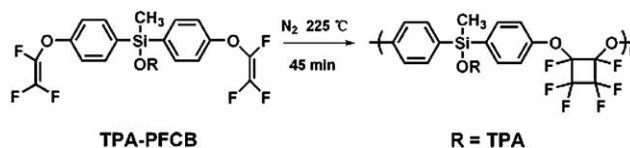
Scheme 1 The molecular structure of TPA–PFCB.

[a]Center for Polymers and Organic Solids, University of California, Santa Barbara, California, 93106, USA. E-mail: ajhe@physics.ucsb.edu
[b]Materials Research Laboratory, Department of Chemistry and Biochemistry, University of California, Santa Barbara, California, 93106, USA

† This paper is part of a *Journal of Materials Chemistry* themed issue in celebration of the 70th birthday of Professor Fred Wudl.
‡ Electronic supplementary information (ESI) available: Experimental details, device fabrication and characterizations, UV absorption spectra and UPS spectra. See DOI: 10.1039/c0jm02224a
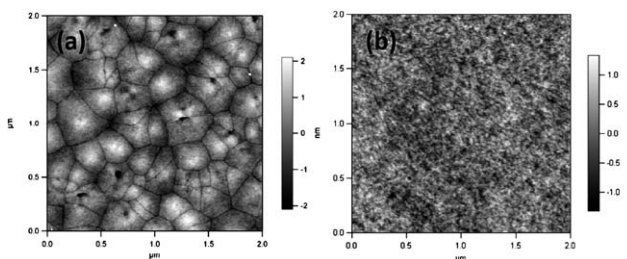

Fig. 1 AFM images of (a) ITO-coated glass substrate and (b) TPA–PFCB thin film on ITO-coated glass substrate. The images were obtained for 2 μm × 2 μm surface area.

This journal is © The Royal Society of Chemistry 2011

J. Mater. Chem., 2011, **21**, 1365–1367 | 1365

To clarify the role of TPA–PFCB as a hole-transport and electron-blocking layer, bipolar field-effect transistors (FETs) and organic solar cells based on poly(3-hexylthiophene-2,5-diyl)/[6,6]-phenyl C$_{61}$ butyric acid methyl ester (P3HT/PCBM) layer were fabricated and characterized.

The FET structure and transfer characteristics are shown in Fig. 2. For the FET without the TPA–PFCB layer, typical bipolar transfer characteristics were found with hole mobility (μ_h) and electron mobility (μ_e) nearly balanced ($\mu_h \approx 0.0011$ cm^2 V^{-1} s^{-1} and $\mu_e \approx 0.0032$ cm^2 V^{-1} s^{-1}). Devices with the TPA–PFCB layer exhibited only hole transport. Compared with the device without the TPA–PFCB layer, the current under positive V_{gs} decreases by more than 3 orders of magnitude. TPA–PFCB is an excellent electron blocker. The highest occupied molecular orbital (HOMO) of TPA–PFCB is at 5.2 eV below the vacuum.[27] The lowest unoccupied molecular orbital (LUMO) can be estimated from the optical gap to be at 1.7 eV. Electron transport is, therefore, blocked because of the large energy gap.

To illustrate the utility of TPA–PFCB as a hole extraction layer, BHJ solar cells were fabricated; the device structure and the energy levels are shown in Fig. 3. Devices based on PEDOT:PSS (device A: ITO/PEDOT:PSS/P3HT:PCBM/Ca/Al) yielded PCE of 3.50%. We found that insertion of a thin PEDOT:PSS layer between the TPA–PFCB and the BHJ layer (device B: ITO/TPA–PFCB/PEDOT:PSS/P3HT:PCBM/Ca/Al) improves the cell performance. The PCE increased to 3.90%. Over ten devices were tested and the average PCEs increased by 0.2%. The current density–voltage (J–V) characteristics of the devices under AM 1.5 G irradiation from a calibrated solar simulator with an irradiation intensity of 100 mW cm^{-2} are shown in Fig. 3c. Compared with the control devices based on PEDOT:PSS as the hole transport layer (*i.e.* without TPA–PFCB), V_{oc} and J_{sc} both increased, leading to the increased PCE. Furthermore, as shown in Fig. 3d, the dark current of device with TPA–PFCB is one order of magnitude lower than that of a similar device without TPA–PFCB. The smaller current density reconfirms the electron blocking effect of TPA–PFCB.
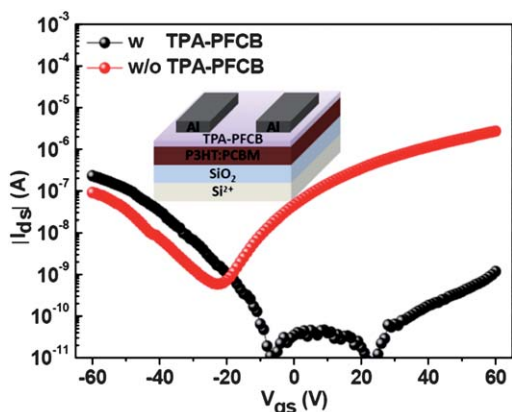

Fig. 3 (a) The device structure of PSCs. (b) The energy level diagram of the components. (c) J–V characteristics of device A: ITO/PEDOT:PSS/P3HT:PCBM/Ca/Al and device B: ITO/TPA–PFCB/PEDOT:PSS/P3HT:PCBM/Ca/Al. The device performance is summarized as follows: the device A shows: $J_{sc} = 9.10$ mA cm^{-2}, $V_{oc} = 0.60$ V, FF = 65%, and PCE = 3.50% and device B shows: $J_{sc} = 9.43$ mA cm^{-2}, $V_{oc} = 0.61$ V, FF = 67%, and PCE = 3.90%. (d) The dark currents of device A and device B.

In summary, we successfully demonstrated TPA–PFCB as a hole-transport and electron-blocking layer. FET measurement showed that electron transport is completely blocked by insertion of TPA–PFCB between the BHJ layer and the Al source and drain electrodes. A thin TPA–PFCB layer inserted between ITO and the BHJ layer in solar cell architecture blocked electrons from travelling to the ITO. Compared with the control solar cells without TPA–PFCB, both V_{oc} and J_{sc} increased, leading to enhanced efficiency.

Acknowledgements

Notes and references

1 N. S. Sariciftci, L. Smilowitz, A. J. Heeger and F. Wudl, *Science*, 1992, **258**, 1474.
2 G. Yu, J. Gao, J. C. Hemmelen, F. Wudl and A. J. Heeger, *Science*, 1995, **270**, 1789.
3 S. Gunes, H. Neugebauer and N. S. Sariciftci, *Chem. Rev.*, 2007, **107**, 1324.
4 P. W. M. Blom, V. D. Mihailetchi, L. J. A. Koster and D. E. Markov, *Adv. Mater.*, 2007, **19**, 1551.
5 G. Dennler, M. C. Scharber and C. J. Brabec, *Adv. Mater.*, 2009, **21**, 1323.
6 L. M. Chen, Z. Hong, G. Li and Y. Yang, *Adv. Mater.*, 2009, **21**, 1434.
7 Y. Liang, Y. Wu, D. Feng, S. T. Tsai, H. J. Son, G. Li and L. Yu, *J. Am. Chem. Soc.*, 2009, **131**, 56.
8 D. Muhlbacher, M. Scharber, M. Morana, Z. Zhu, D. Waller, R. Gaudiana and C. Brabec, *Adv. Mater.*, 2006, **18**, 2884.
9 N. Blouin, A. Michaud, D. Gendron, S. Wakim, E. Blair, R. Neagu-Plesu, M. Bellêtête, G. Durocher, Y. Tao and M. Leclerc, *J. Am. Chem. Soc.*, 2008, **130**, 732.
10 M. C. Scharber, M. Koppe, J. Gao, F. Cordella, M. A. Loi, P. Denk, M. Morana, H. J. Egelhaaf, K. Forberich, G. Dennler, R. Gaudiana, D. Waller, Z. Zhu, X. Shi and C. J. Brabec, *Adv. Mater.*, 2006, **22**, 367.

Fig. 2 Transfer characteristics of bipolar FETs based on P3HT/PCBM blend with TPA–PFCB and without TPA–PFCB on the top. Drain current (I_{ds}) under negative gate voltage (V_{gs}) indicates the hole transport (left-hand side); drain current under positive gate voltage indicates the electron transport (right-hand side). The applied drain–source voltage (V_{ds}) was consistent (−60 V) and V_{gs} was applied from 60 V to −60 V. The inset shows the device structure of bipolar FETs.
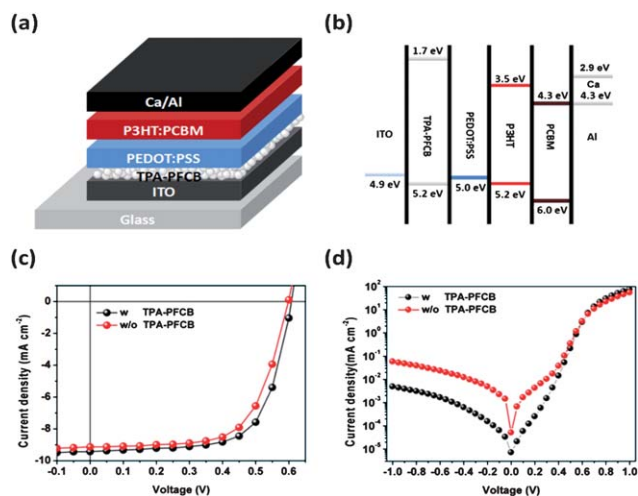
11 R. C. Coffin, J. Peet, J. Rogers and G. C. Bazan, *Nat. Chem.*, 2009, **1**, 657.

12 W. L. Ma, C. Y. Yang, X. Gong, K. Lee and A. J. Heeger, *Adv. Funct. Mater.*, 2005, **15**, 1617.

13 G. Li, V. Shrotriya, J. Huang, Y. Yao, T. Moriarty, K. Emery and Y. Yang, *Nat. Mater.*, 2005, **4**, 864.

14 F. Padinger, R. S. Rittberger and N. S. Sariciftci, *Adv. Funct. Mater.*, 2003, **13**, 85.

15 F. Zhang, K. G. Jespersen, C. Björström, M. Svensson, M. R. Andersson, V. Sundström, K. Magnusson, E. Moons, A. Yartsev and O. Inganäs, *Adv. Funct. Mater.*, 2006, **16**, 667.

16 J. Peet, J. Y. Kim, N. E. Coates, W. L. Ma, D. Moses, A. J. Heeger and G. C. Bazan, *Nat. Mater.*, 2007, **6**, 497.

17 X. Gong, M. Tong, Y. Xia, W. Cai, J. S. Moon, Y. Cao, G. Yu, C.-L. Shieh, B. Nisson and A. J. Heeger, *Science*, 2009, **325**, 1665.

18 S. H. Park, A. Roy, S. Beaupre, S. Cho, N. Coates, J. S. Moon, D. Moses, M. Leclerc, K. Lee and A. J. Heeger, *Nat. Photonics*, 2009, **3**, 297.

19 J. Y. Kim, S. H. Kim, H.-H. Lee, K. Lee, W. L. Ma, X. Gong and A. J. Heeger, *Adv. Mater.*, 2006, **18**, 572.

20 J. Y. Kim, K. Lee, N. E. Coates, D. Moses, T. Q. Nguyen, M. Dante and A. J. Heeger, *Science*, 2007, **317**, 222.

21 A. Roy, S. H. Park, S. Cowan, M. H. Tong, S. Cho, K. Lee and A. J. Heeger, *Appl. Phys. Lett.*, 2009, **95**, 013302.

22 R. Steim, F. R. Kogler and C. J. Brabec, *J. Mater. Chem.*, 2010, **20**, 2499.

23 P. Peumans and S. R. Forrest, *Appl. Phys. Lett.*, 2001, **79**, 126.

24 K. Takahashi, S. Suzaka, Y. Sigeyama, T. Yamaguchi, J. I. Nakamura and K. Murata, *Chem. Lett.*, 2007, **36**, 762.

25 A. W. Hains and T. J. Marks, *Appl. Phys. Lett.*, 2008, **92**, 023504.

26 H. Yan, P. Lee, A. G. Armstrong, G. A. Evmenenko, P. Dutta and T. J. Marks, *J. Am. Chem. Soc.*, 2005, **127**, 3172.

27 F. Huang, Y. J. Cheng, Y. Zhang, M. S. Liu and A. K. Y. Jen, *J. Mater. Chem.*, 2008, **18**, 4495.